



OPEN Effects of different ventilatory settings on alveolar and pulmonary microvessel dimensions in pigs

Elisa Damiani^{1,2}✉, Erika Casarotta¹, Caterina Di Bella³, Margherita Galosi³, Alessio Angorini³, Federica Serino³, Adolfo Maria Tambella³, Fulvio Laus³, Samuele Zuccari², Alessio Salvucci Salice¹, Roberta Domizi^{1,2}, Andrea Carsetti^{1,2}, Can Ince⁴ & Abele Donati^{1,2}

Mechanical ventilation with high tidal volume (TV) or positive end-expiratory pressure (PEEP) may induce lung overinflation and increased pulmonary vascular resistance to flow. In 8 healthy mechanically ventilated pigs, we evaluated whether incident dark field (IDF) vital microscopy, applied through a small thoracotomy, could be used to evaluate changes in alveolar and pulmonary microvessel dimensions under different ventilator settings. High TV (12 ml/kg) increased alveolar diameters (from 99 ± 13 to $114 \pm 6 \mu\text{m}$, $p < 0.05$ repeated measures one way analysis of variance) and reduced septal capillary diameters (from 12.1 ± 1.7 to $10.5 \pm 1.4 \mu\text{m}$, $p < 0.001$) as compared to 8 ml/kg TV. This effect was more pronounced in non-dependent lung. Alveolar and microvessel diameters did not change with high PEEP (12 cmH₂O Vs. 5 cmH₂O). High FiO₂ (100%) led to pulmonary vasodilation (from 12.1 ± 1.7 to $14.7 \pm 1.4 \mu\text{m}$, $p < 0.001$), with no change in alveolar dimensions as compared to 50% FiO₂. In conclusion, IDF imaging enabled to obtain high-quality images of subpleural alveoli and microvessels. High TV ventilation may induce alveolar distension with compression of septal capillaries, thus potentially increasing dead space ventilation.

Keywords Mechanical ventilation, Pulmonary microcirculation, Ventilation/perfusion matching, Incident dark field, Hand-held vital microscopy

Mechanical ventilation is an essential supportive therapy in the treatment of patients with acute respiratory failure to improve gas exchange and reduce the work of breathing. However, ventilatory settings need to be finely modulated to respect the pulmonary mechanics in healthy or injured lungs. Mechanical ventilation may cause pulmonary structural damage, known as ventilator-induced lung injury (VILI)¹. High tidal volume (TV) ventilation may induce volutrauma, i.e. tissue damage caused by excessive stretching of lung tissues that occurs when the lung is over-inflated. Protective ventilation strategies using low TV led to better outcome in mechanically ventilated patients with acute respiratory distress syndrome². Positive end-expiratory pressure (PEEP) improves oxygenation by recruiting collapsed alveoli and increasing alveolar stability³. Nonetheless, higher PEEP levels may also enhance static stress and increase the risk of over-inflation³. Alveolar over-inflation, besides inducing barotrauma/volutrauma, can cause stretching and compression of pulmonary capillaries with increased pulmonary vascular resistance to flow^{4,5}. These effects could manifest themselves maximally in non-dependent lung areas, where higher TV or PEEP may increase wasted ventilation towards non-dependent poorly perfused regions and redistribute perfusion towards dependent poorly ventilated areas, thereby worsening the ventilation-perfusion matching and gas-exchange^{6,7}.

The use of intravital microscopy for the assessment of alveolar anatomy and mechanics in animal models has provided relevant insights into the pathophysiology of mechanical ventilation and VILI^{6,8}. More recently, sidestream dark field (SDF) imaging has been applied in a few studies to evaluate pulmonary microcirculation under mechanical ventilation in canine or porcine models^{9,10}. By using SDF imaging, den Uil et al. were able to visualize the subpleural alveoli and analyze their dimensions in patients undergoing elective cardiac surgery¹¹.

We performed a feasibility study, aiming to explore whether incident dark field (IDF) intravital microscopy could be used to visualize and measure alveolar and pulmonary microvessel diameters in mechanically ventilated pigs. Moreover, we tested the hypothesis that higher TV or PEEP may induce an increase in alveolar size (over-

¹Department of Biomedical Sciences and Public Health, Università Politecnica delle Marche, via Trontrò 10/a, 60126 Ancona, Italy. ²Anesthesia and Intensive Care Unit, Azienda Ospedaliero Universitaria delle Marche, Ancona, Italy. ³School of Biosciences and Veterinary Medicine, University of Camerino, Camerino, Italy. ⁴Department of Intensive Care, Erasmus MC, University Medical Center, Rotterdam, The Netherlands. ✉email: elisa.damiani@univpm.it

	Average value at baseline (TV 8 ml/kg, PEEP 5 cmH ₂ O, FiO ₂ 0.5)
Temperature (°C)	36.6 ± 0.7
Mean arterial pressure (mmHg)	89 ± 19
Heart rate (bpm)	114 ± 32
Respiratory rate (breaths/min)	27 ± 9
Hemoglobin (g/dL)	9.9 ± 1.3
Arterial pH	7.43 ± 0.08
Arterial PO ₂ (mmHg)	199 ± 36
Arterial PCO ₂ (mmHg)	47 ± 10
PaO ₂ /FiO ₂ (mmHg)	397 ± 72

Table 1. General data at baseline. Data are expressed as mean ± standard deviation. *Bpm* beats per minute, *PaO₂* arterial oxygen tension, *PaCO₂* carbon dioxide tension, *FiO₂* inspiratory oxygen fraction.

	TV 8 ml/kg PEEP 5 cmH ₂ O FiO ₂ 0.5	TV 12 ml/kg PEEP 5 cmH ₂ O FiO ₂ 0.5	TV 8 ml/kg PEEP 12 cmH ₂ O FiO ₂ 0.5	TV 8 ml/kg PEEP 5 cmH ₂ O FiO ₂ 1.0	<i>p</i> (overall)
Static compliance (ml/cmH ₂ O)	47 [26–56]	38 [28–53]	33 [23–41]	47 [37–54]	0.088
Plateau Pressure (cmH ₂ O)	11 [10–14]	15 [14–16]	20 [19.7–21]**	11 [10–12]	<0.001
Driving Pressure (cmH ₂ O)	6 [5–9]	10 [9–11]*	8 [7.7–9]	6 [5–7]	0.001

Table 2. Respiratory mechanics at different ventilator settings. **p* < 0.05, ***p* < 0.01 Vs. baseline, Friedman test with multiple comparisons. Data are expressed as median [1st–3rd quartile]. *TV* tidal volume, *PEEP* positive end-expiratory pressure, *FiO₂* inspiratory oxygen fraction.

inflation) and a decrease in vessel diameter. We further evaluated the impact of higher FiO₂ on alveoli and pulmonary microvessels to test the hypothesis that hyperoxia may induce a visible vasodilation in the pulmonary circulation¹².

Results

General hemodynamic and respiratory data at baseline ventilatory settings are shown in Table 1. Changes in respiratory mechanics at different ventilatory settings are reported in Table 2. The increase in TV from 8 ml/kg to 12 ml/kg induced an increase in the Driving Pressure, while the increase in PEEP from 5 cmH₂O to 12 cmH₂O induced an increase in the Plateau Pressure (Table 2). No significant variation in static compliance was found (Table 2).

Changes in ventilator settings led to significant variations in mean alveolar diameters (*p* = 0.046, repeated measures one-way analysis of variance [ANOVA]) and mean pulmonary vessel diameters (*p* < 0.001) (Fig. 1). The increase in TV from 8 ml/kg to 12 ml/kg tended to increase the mean alveolar diameter from 99 ± 13 μm to 114 ± 6 μm (*p* = 0.115 Vs. baseline, Holm-Sidak's multiple comparison test) and reduce the mean vessel diameter from 12.1 ± 1.7 μm to 10.5 ± 1.4 μm (*p* = 0.018). The increase in the FiO₂ to 1.0 induced a vasodilation in the pulmonary microcirculation, with an increase in the mean vessel diameter from 12.1 ± 1.7 μm to 14.7 ± 1.4 μm (*p* = 0.003). Changes in mean alveolar or vessel diameters with the increase in PEEP from 5 cmH₂O to 12 cmH₂O were not significant.

Table 3 shows a comparison in mean alveolar and vessel diameters between non-dependent and dependent lung regions, and their changes with different ventilator settings. Mean alveolar diameters tended to be lower in dependent lung areas (*p* = 0.013, two-way ANOVA). The increase in TV induced alveolar distension in both non-dependent (*p* = 0.092, Holm-Sidak's multiple comparisons test) and dependent areas (*p* = 0.026), whereas it led to a significant reduction in vessel diameters only in non-dependent lung regions (*p* < 0.001). The increase in PEEP did not produce significant changes in alveolar or vessel diameters in either non-dependent or dependent lung regions. Ventilation with an FiO₂ of 1.0 led to an increase in vessel diameters in both non-dependent (*p* = 0.003) and dependent areas (*p* < 0.001).

We found no correlation between percentage changes in lung mechanics and changes in mean alveolar diameters induced by different ventilator settings (Fig. 2). On the contrary, changes in Plateau Pressure or Driving Pressure were inversely related with changes in pulmonary vessel diameter and positive correlations were found between changes in static compliance and changes in vessel diameters (Fig. 2).

Discussion

We applied IDF vital microscopy on the lungs of mechanically ventilated pigs to test the hypothesis that different ventilator settings may alter alveolar and microvessel dimensions, thus potentially modifying ventilation/perfusion matching. Our study shows that: high TV (12 ml/kg as compared to 8 ml/kg) induces an increase in alveolar dimensions but a reduction in microvessel diameters, while high PEEP (12 cmH₂O as compared to 5 cmH₂O) did not induce visible changes in either alveolar or microvessel diameters; the effect of high TV on

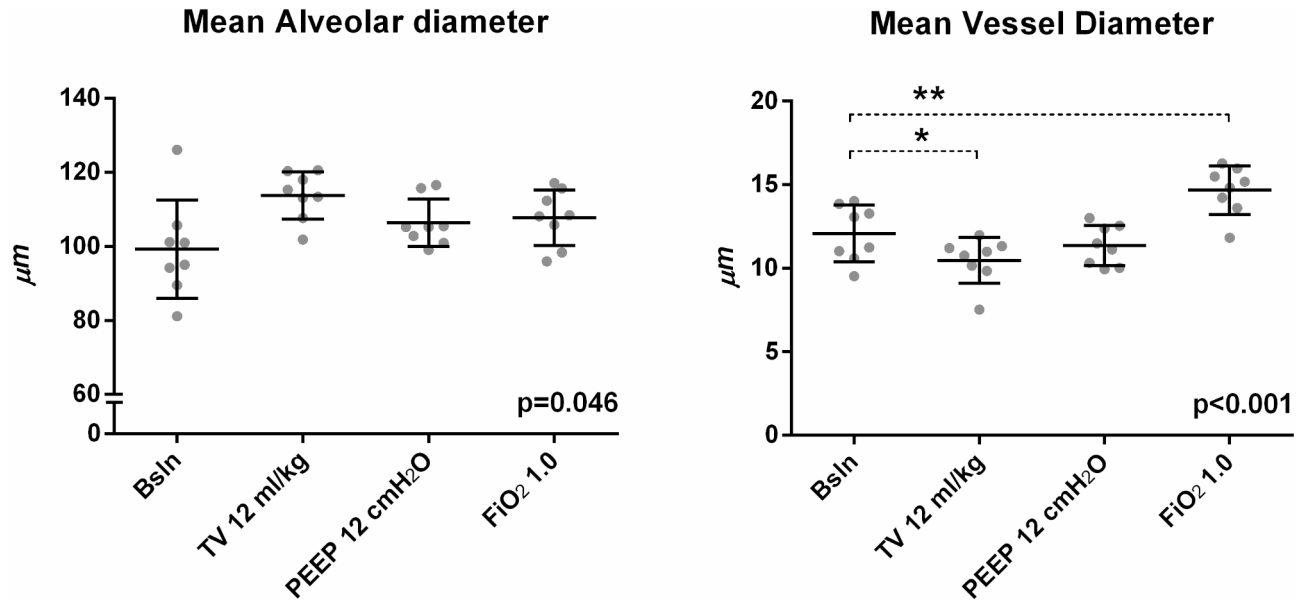


Fig. 1. Changes in mean alveolar diameters and microvessel diameters with different ventilatory settings. * $p < 0.05$, ** $p < 0.01$, repeated measures one-way ANOVA with Holm-Sidak's multiple comparison test and Geisser-Greenhouse correction.

		TV 8 ml/kg PEEP 5 cmH ₂ O FiO ₂ 0.5	TV 12 ml/kg PEEP 5 cmH ₂ O FiO ₂ 0.5	TV 8 ml/kg PEEP 12 cmH ₂ O FiO ₂ 0.5	TV 8 ml/kg PEEP 5 cmH ₂ O FiO ₂ 1.0	<i>p</i> (for interaction)	<i>p</i> (for ventilator setting)	<i>p</i> (for lung area)
Mean Alveolar diameter (µm)	Non-dependent lung	105 ± 20	118 ± 12	109 ± 9	114 ± 9	0.827	0.011	0.013
	Dependent lung	93 ± 11	109 ± 11*	104 ± 10	102 ± 11			
Mean Vessel diameter (µm)	Non-dependent lung	12.1 ± 2.2	9.7 ± 1.6***	11.4 ± 1.3	14.2 ± 2.2**	0.161	<0.001	0.369
	Dependent lung	12.0 ± 1.5	11.3 ± 1.7	11.3 ± 1.3	15.2 ± 1.3***			
Alveoli (nr/µm ²)	Non-dependent lung	49 ± 13	43 ± 14	50 ± 18	50 ± 11	0.626	0.690	0.579
	Dependent lung	46 ± 24	44 ± 9	44 ± 17	42 ± 19			

Table 3. Changes in pulmonary alveoli and microvessels at different ventilatory settings. * $p < 0.05$ Vs. baseline, two-way ANOVA with Holm-Sidak's multiple comparisons test and the Geisser-Greenhouse correction. Data are expressed as mean ± standard deviation. TV tidal volume, PEEP positive end-expiratory pressure, FiO₂ inspiratory oxygen fraction.

vessel diameters was mainly observed in non-dependent areas; hyperoxia (FiO₂ 1.0 as compared to 0.5) induces vasodilation in the pulmonary microcirculation.

High TV ventilation contributes to VILI by inducing alveolar overdistension due to increased transpulmonary pressure (volutrauma) and lung inflammation (biotrauma)¹³. By using isolated ventilated rat lungs perfused with fluorescent latex microparticles, Conhaim et al. showed that under positive pressure ventilation the pulmonary acinar microvessels are compressed and blood bypasses the alveolar capillaries flowing through larger septal intrapulmonary vessels¹⁴. Using a similar model, Tanabe et al. demonstrated that an increase in airway pressure led to a derecruitment in septal capillaries and a more homogeneous venular flow (due to blood flow arterio-venular shunting)¹⁵. Our findings are consistent with these data. Ventilation with 12 ml/kg TV led to alveolar distension and compression of septal microvessels, which showed significantly lower diameters. Importantly, microvessel diameters were particularly reduced in non-dependent lung areas, where the alveoli were more inflated. In a rat model of injurious ventilation with high peak inspiratory pressure and low PEEP, alveolar injury developed earlier in non-dependent lung regions: these areas have higher compliance and normally receive a larger percentage of the TV as compared with the dependent lung⁶. These data underline an important concept: alveolar overdistension due to high-TV ventilation in normally aerated lung regions will compromise capillary perfusion in the same areas, thereby increasing the dead space ventilation and worsening oxygenation. In addition, pulmonary vascular resistance and right ventricular afterload will increase, with potential hemodynamic compromise.

Ventilation with high PEEP (12 cmH₂O as compared to 5 cmH₂O) produced no overall change in alveolar diameters in our model of mechanically ventilated pigs with healthy lungs, despite inducing an increase in Plateau Pressure. However, even if differences were not significant, alveolar diameters tended to be higher in

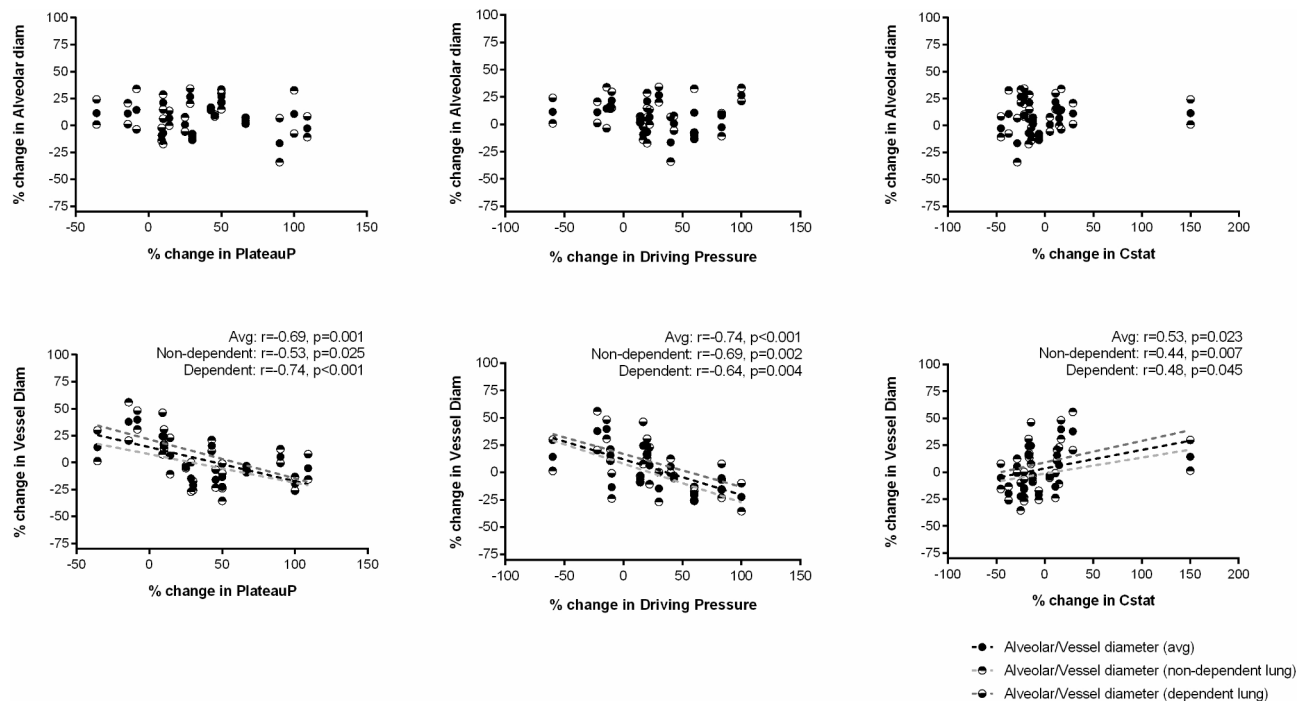


Fig. 2. Correlations between percentage changes in plateau pressure, driving pressure and static compliance and percentage changes in alveolar and microvessel diameters. Correlations were explored separately for all alveoli/microvessels (full black dots), non-dependent alveoli/microvessels (upper black dots) and dependent alveoli/microvessels (lower black dots).

dependent areas with high PEEP: this would suggest a more uniform distribution of the TV. These data support the concept that optimal PEEP levels increase alveolar stability and limit derecruitment (atelectrauma) rather than inducing alveolar overinflation¹⁶. More importantly, in our study high PEEP did not induce significant changes in microvessel diameters. This seems in contrast with other studies. By using *in vivo* photomicroscopy in dogs, Nieman et al. showed that the application of 15 cmH₂O PEEP reduced the cardiac output and alveolar capillary perfusion; restoration of cardiac output with volume expansion failed to restore alveolar perfusion to baseline values, supporting the hypothesis that PEEP impairs pulmonary microvasculature mainly through direct compression¹⁷. Similar results were found by He et al. with the application of 25 cmH₂O PEEP⁹. In mechanically ventilated pigs with low cardiac output, Pan et al. showed an impairment in pulmonary microvascular flow under increasing PEEP levels (up to 20 cmH₂O) with periodic collapse of pulmonary capillaries at inspiration; these blood flow alterations were not observed in pigs receiving dobutamine to maintain a high cardiac output¹⁰. These data emphasize the role of heart/lung interactions and the possible impact of positive pressure ventilation on hemodynamics and lung perfusion, especially in presence of hypovolemia. Even if we did not calculate parameters of microvascular flow quality, blood flow appeared continuous in septal capillaries in all animals, with no evidence of obstruction independently of TV, PEEP or FiO₂. In our study, the lack of flow impairment or reduction in pulmonary vessel diameters with high PEEP may be explained by several factors. First, we used a 12 cmH₂O PEEP level, lower than PEEP levels used in other studies^{9,10,17}. Second, euvoolemia in our model was maintained through a continuous fluid infusion: an optimal cardiac output could have prevented a reduction in pulmonary blood flow under high PEEP. Third, our analysis was focused on septal capillaries; we cannot exclude that high PEEP caused compression and collapse of smaller acinar microvessels, as these were not explorable.

Oxygen exerts important effects on lung physiology. An increase in alveolar PO₂ acts as a potent and selective pulmonary vasodilator: the underlying mechanisms include endothelial hyperpolarization and release of vasodilating molecules that act by reducing the intracellular calcium concentration in the vascular smooth cells¹². For this reason, a possible role of oxygen has been postulated for treating pulmonary arterial hypertension, although current guidelines recommend its use only for patients with severe hypoxemia¹². In this study, we were able to show an increase in pulmonary microvessel diameters following exposure to 1.0 FiO₂. Oxygen may also exert toxic effects on the lungs. Hyperoxia-induced lung injury includes oxidative stress and inflammation, impaired surfactant production with alveolar instability and resorption atelectasis¹⁸. In a randomized trial on patients undergoing abdominal surgery, the administration of higher FiO₂ during anesthesia and recovery increased postoperative atelectasis¹⁹. In our experiments with short-term exposure to hyperoxia, we did not observe any variation in alveolar diameters: more prolonged exposures are likely required to induce alveolar derecruitment.

This study has several limitations. First, we evaluated the pulmonary alveoli and microvessels only after a short period of mechanical ventilation: ventilation for longer time periods would likely increase atelectasis in dependent lung areas and influence the response to high TV or PEEP. Nonetheless, it is important to note

that significant differences in alveolar diameters were found between non-dependent and dependent regions only after a 30-minute period of mechanical ventilation. Second, measurements were taken only 3–5 min after the variations in ventilatory settings. Even if it would be interesting to explore the possible injurious effects of high-TV ventilation or the impact of high PEEP after longer exposures, the goal of our analysis was to describe the acute changes of alveolar and pulmonary vessel dimensions under different ventilator settings. Moreover, we followed the same sequence of ventilatory settings for all pigs, and cannot totally exclude that the alveolar/microvessel diameters observed at each time-point were somehow influenced by the previous settings. Third, IDF imaging was applied during expiratory holds. We did not evaluate the dynamic changes of alveoli/microvessels during inflation/deflation¹⁶; we acknowledge that such evaluation could have provided relevant insights on alveolar stability. Moreover, at end-expiration the effects of high TV (or high PEEP) were likely underestimated: we could have found a more pronounced alveolar distension at end-inspiration with more severe compression of septal capillaries and blood flow obstruction¹⁰. Fourth, we were able to describe only changes in subpleural alveoli and microvessels, which may differ from those occurring in inner regions. Fifth, with the handheld IDF device intermittently applied on the pleural surface, we were not able to track the same anatomical structures during changes in ventilator settings. This may have increased the variability in the response observed. However, by taking measurements of dependent and non-dependent lung regions, we aimed to analyze the two parts of the lung with the highest expected difference in ventilation/perfusion ratio. Sixth, we did not measure the cardiac output and its variations under high TV, PEEP or FiO₂: this could have provided relevant information on heart-lung interaction and the hemodynamic impact of different ventilatory settings. Lastly, we evaluated healthy lungs. It would be interesting to explore the effects of high TV, high PEEP or high FiO₂ on alveoli and pulmonary microvasculature in heterogeneously injured lungs (such as in ARDS).

In conclusion, in mechanically ventilated pigs with healthy lungs, ventilation with high TV induced alveolar distension and compression of septal capillaries. This effect was more pronounced in non-dependent lung regions and may increase dead space ventilation. In this study, alveolar diameters did not change significantly and pulmonary microvessels were unaffected by the administration of 12 cmH₂O PEEP. Hyperoxia led to pulmonary vasodilation, with no change in alveolar dimensions. The application of IDF imaging to observe the pulmonary alveoli and microcirculation in animal models may provide relevant insights into ventilation-perfusion matching and pulmonary hemodynamics.

Methods

The study protocol was approved by the Italian Ministry of Health (Ministero della Salute – Direzione Generale della Sanità Animale e dei Farmaci Veterinari), authorization number 701/2023-PR, protocol nr. E81AC.18, 31st July 2023. All experiments were performed in accordance with the relevant guidelines and regulations, and reported in compliance with the ARRIVE guidelines.

Eight healthy pigs (3 males, 5 females) weighing 31 (29–35) kg were used. After a 12-hour fasting with free access to water, pigs were sedated with a 0.02–0.04 ml/kg intramuscular injection of tiletamine/zolazepam (50/50 mg/ml) plus xylazine 250 mg (2.5 ml) plus ketamine 250 mg (2.5 ml). An auricular venous access was placed and anesthesia was induced by intravenous injection of fentanyl (1 µg/kg) plus propofol (5 mg/kg). The trachea was intubated with a cuffed endotracheal tube (anterior diameter of 7.0 mm), the animal was placed in supine position and connected to the mechanical ventilator (Datex Ohmeda S/5 Aespire, Florida, USA) in volume controlled mode with 8 ml/kg TV, inspiration: expiration ratio of 1:2, PEEP of 5 cmH₂O and FiO₂ 0.5. The respiratory rate (RR) was set to obtain an end-tidal CO₂ of 35–40 mmHg. Anesthesia was maintained with intravenous infusions of propofol (0.1–0.2 mg/kg/min), dexmedetomidine (1 µg/kg/h), fentanyl (10–20 µg/kg/h) and rocuronium (0.4 mg/kg/h). SpO₂ was monitored with tongue pulse oxymetry. The femoral artery was cannulated for continuous arterial pressure monitoring and blood gas analysis (Idexx VetStat[®], Idexx Laboratories Italia Srl, Milano, Italy). During the experiment, the animals received a continuous intravenous infusion of crystalloids (10 ml/kg/h). Norepinephrine was administered to maintain a mean arterial pressure ≥65 mmHg, as needed. Measurements were taken after a 30-minutes period of stabilization.

Assessment of lung alveoli and microvessels

A 5-cm thoracotomy was performed on the left lower thoracic wall along the mid-axillary line. The subpleural alveoli and microcirculation were visualized using IDF imaging (Cytocam-IDF, Braedius Medical, Amsterdam, The Netherlands). This is a hand-held vital microscope enabling the real-time in vivo visualization of the microcirculation, especially in the sublingual mucosa of critically ill patients²⁰. Briefly, IDF-imaging consists of an illumination unit with a 4x magnification lens. The light is emitted at a wavelength of 548 nm, ensuring the absorption by oxy- and deoxy-hemoglobin, whereby flowing red blood cells can be visualized as dark moving globules against a clear background²¹. Herein, we used this device as an intravital microscope to obtain two-dimensional images of pulmonary structures. Subpleural alveoli and inter-alveolar septal capillaries can be visualized due to the reflection of the emitted light by alveolar walls¹¹. The tip of the Cytocam, covered with a sterile disposable cap, was inserted through the thoracotomy and placed in contact with the pleural surface. During expiration holds periods (10 s)^{9,10}, two videos of the subpleural alveoli/microcirculation were recorded with adequate focus and contrast in non-dependent and dependent lung regions, respectively, by moving the probe towards the anterior and posterior lung regions. Videos were analyzed offline using the Automated Vascular Analysis software package (AVA version 3.2, Microvision Medical, Amsterdam, The Netherlands). The outer walls of the individual alveoli were manually traced and the alveolar circumferences were recorded. Alveolar diameters were calculated dividing the circumferences by π . All visible septal microvessels were identified and their diameters were recorded (Fig. 3).

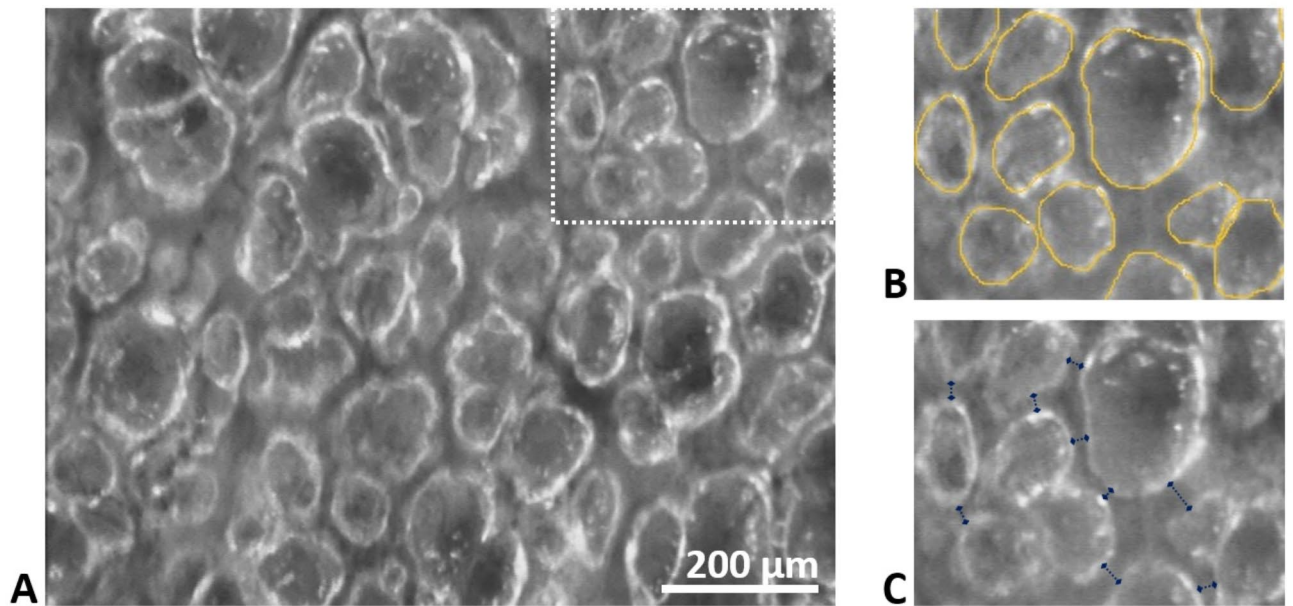


Fig. 3. Example of pulmonary alveoli and microvessels as visualized through IDF videomicroscopy. (A) The light emitted by the Cytocam-IDF probe is reflected by the alveolar walls, which appear as a white line along the outer alveolar perimeter. The light is absorbed by hemoglobin in red blood cells, so that septal capillaries appear in dark grey color. Smaller acinar microvessels were not accurately explorable, therefore our analysis was focused on septal vessels. (B) Example analysis of alveolar dimensions in a segment of the whole image shown in A: yellow lines indicate the alveolar perimeters; the average diameters were then calculated by dividing the perimeters by π . (C) Blue arrows indicate septal microvessel diameters.

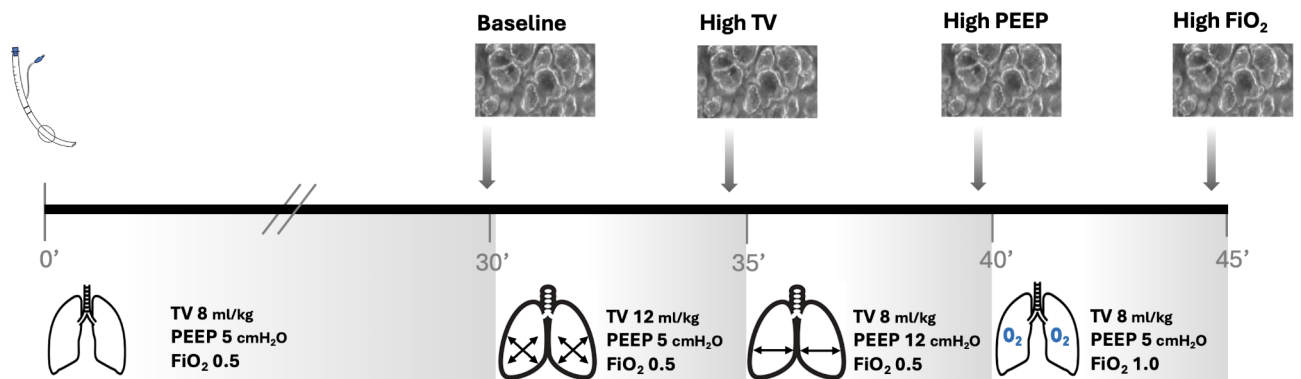


Fig. 4. Experimental protocol.

Experimental protocol

IDF imaging was performed: at *baseline* ventilatory settings, with TV 8 ml/kg, PEEP 5 cmH₂O, FiO₂ 0.5; at *high TV*: TV 12 ml/kg, PEEP 5 cmH₂O, FiO₂ 0.5; at *high PEEP*: TV 8 ml/kg, PEEP 12 cmH₂O, FiO₂ 0.5; at *high FiO₂*: TV 8 ml/kg, PEEP 5 cmH₂O, FiO₂ 1.0 (Fig. 4). Measurements were taken at least 3 min after modifying the ventilator settings. Respiratory mechanics was assessed at each time point, as follows: the plateau pressure was measured at end-inspiration during an inspiratory hold, the driving pressure was calculated as the difference between the plateau pressure and PEEP, static compliance was calculated dividing the TV by the driving pressure. Pigs were then used for subsequent experiments (no other procedures or measurements were taken before the ones described in the present study). Adequate anesthesia and analgesia were provided throughout the whole duration of the experimental procedures. Pigs were finally euthanized with an intravenous overdose of potassium chloride.

Statistical analysis

This was performed using GraphPad Prism version 6 (GraphPad software, La Jolla, CA, USA). Normality of distribution was checked using the Kolmogorov-Smirnov test. Data were expressed as mean \pm standard deviation or median [1st -3rd quartiles], as appropriate. We used a repeated-measures one-way ANOVA with

the Holm-Sidak's multiple comparisons test and the Geisser-Greenhouse correction to evaluate the effect of different ventilator settings on alveolar or vessel diameters. A Friedman test with Dunn's multiple comparisons test was used for non-normally distributed variables. To test the effects of ventilator settings or lung area on alveolar/vessel diameters, we applied a repeated measures two-way ANOVA with the Holm-Sidak's multiple comparisons test and the Geisser-Greenhouse correction to compare data from non-dependent and dependent lung regions. The Spearman's rho was calculated to test the correlation between percentage variations in lung mechanics (driving pressure, plateau pressure, static compliance) and percentage variations in alveolar/vessel diameters. A two-tailed $p < 0.05$ was used to define statistical significance.

Data availability

All data is provided within the manuscript.

Received: 27 September 2024; Accepted: 3 December 2024

Published online: 05 December 2024

References

- Silva, P. L., Scharffenberg, M. & Rocco, P. R. M. Understanding the mechanisms of ventilator-induced lung injury using animal models. *Intensive Care Med. Exp.* **11**, 82 (2023).
- Network, A. R. D. S. et al. Ventilation with lower tidal volumes as compared with traditional tidal volumes for acute lung injury and the acute respiratory distress syndrome. *New Engl. J. Med.* **342**, 1301–1308 (2000).
- Grothberg, J. C., Reynolds, D. & Kraft, B. D. Management of acute respiratory distress syndrome: a primer. *Crit. Care.* **27**, 289 (2023).
- Whittenberger, J. L., McGregor, M., Berglund, E. & Borst, H. G. Influence of state of inflation of the lung on pulmonary vascular resistance. *J. Appl. Physiol.* **15**, 878–882 (1960).
- Assimacopoulos, A., Guggenheim, R. & Kapanci, Y. Changes in alveolar capillary configuration at different levels of lung inflation in the rat. An ultrastructural and morphometric study. *Lab. Invest.* **34**, 10–22 (1976).
- Pavone, L., Albert, S., DiRocco, J., Gatto, L. & Nieman, G. Alveolar instability caused by mechanical ventilation initially damages the nondependent normal lung. *Crit. Care.* **11**, R104 (2007).
- Karbing, D. S. et al. Changes in shunt, ventilation/perfusion mismatch, and lung aeration with PEEP in patients with ARDS: A prospective single-arm interventional study. *Crit. Care.* **24**, 111 (2020).
- Tabuchi, A., Mertens, M., Kuppe, H., Pries, A. R. & Kuebler, W. M. Intravital microscopy of the murine pulmonary microcirculation. *J. Appl. Physiol.* **104**, 338–346 (2008).
- He, H. et al. Effects of high PEEP and fluid administration on systemic circulation, pulmonary microcirculation, and alveoli in a canine model. *J. Appl. Physiol.* **127**, 40–46 (2019).
- Pan, P. et al. Physiological regulation of pulmonary microcirculation under mechanical ventilation at different cardiac outputs and positive end-expiratory pressures in a porcine model. *J. Pers. Med.* **13**, 107 (2023).
- Den Uil, C. A. et al. Intra-operative assessment of human pulmonary alveoli in vivo using Sidestream Dark Field Imaging: A feasibility study. *Med. Sci. Monit.* **15**, MT137–141 (2009).
- Green, S. & Stuart, D. Oxygen and pulmonary artery hypertension: effects, mechanisms and therapeutic benefits. *Eur. J. Prev. Cardiol.* **28**, 127–136 (2021).
- Ziaka, M. et al. High-tidal-volume mechanical ventilation and lung inflammation in intensive care patients with normal lungs. *Am. J. Crit. Care.* **29**, 15–21 (2020).
- Conhaim, R. L., Segal, G. S. & Watson, K. E. Positive pressure ventilation compresses pulmonary acinar microvessels but not their supply vessels. *Microv. Res.* **122**, 71–77 (2019).
- Tanabe, N. et al. Presson, RG. Jr. Role of positive airway pressure on pulmonary acinar perfusion heterogeneity. *J. Appl. Physiol.* **89**, 1943–1948 (2000).
- Halter, J. M. et al. Effect of positive end-expiratory pressure and tidal volume on lung injury induced by alveolar instability. *Crit. Care.* **11**, R20 (2007).
- Nieman, G. F., Paskanik, A. M. & Bredenberg, C. E. Effect of positive end-expiratory pressure on alveolar capillary perfusion. *J. Thorac. Cardiovasc. Surg.* **95**, 712–716 (1988).
- Damiani, E., Donati, A. & Girardis, M. Oxygen in the critically ill: friend or foe? *Curr. Opin. Anaesthesiol.* **31**, 129–135 (2018).
- Park, M. et al. Perioperative high inspired oxygen fraction induces atelectasis in patients undergoing abdominal surgery: a randomized controlled trial. *J. Clin. Anesth.* **72**, 110285 (2021).
- Damiani, E. et al. Microcirculation-guided resuscitation in sepsis: the next frontier? *Front. Med. (Lausanne)*. **10**, 1212321 (2023).
- Aykt, G., Veenstra, G., Scorcella, C., Ince, C. & Boerma, C. Cytocam-IDF (Incident Dark Field Illumination) imaging for bedside monitoring of the microcirculation. *Intensive Care Med. Exp.* **3**, 40 (2015).

Author contributions

E.D., E.C., C.D.B. contributed to the conception and design of the study, acquisition, analysis and interpretation of the data, and drafted the manuscript. M.G., A.A., F.S., A.M.T., S.Z., A.S.S. contributed to the acquisition and analysis of the data and revised the manuscript. F.L., R.D., A.C., C.I., A.D. contributed to the design of the study and interpretation of the data and revised the manuscript critically for important intellectual content. All authors gave final approval of the version of the manuscript submitted for publication. All authors agreed to be accountable for all aspects of the work in ensuring that questions related to the accuracy or integrity of any part of the work are appropriately investigated and resolved.

Declarations

Competing interests

Dr. Ince developed sidestream darkfield imaging and is listed as the inventor on related patents commercialized by MicroVision Medical under a license from the Academic Medical Center. He receives no royalties or benefits from this license. He has been a consultant for MicroVision Medical in the past but has not been involved with this company for more than 5 years now and holds no shares or stock. Braedius Medical, a company owned by a relative of Dr. Ince, developed and designed a handheld microscope, the Cytocam based on incident darkfield imaging, that was used in this study. Dr. Ince has no financial relationship with Braedius

Medical of any sort and has never owned shares, or received consultancy or speaker fees from Braedius Medical. Dr. Ince is the CSO of Active Medical BV, Leiden, The Netherlands, a company that provides devices (OxyCam), software (MicroTools), education (Microcirculation Academy), and services related to clinical microcirculation. All the other authors have no conflicts of interests to declare in relation to this manuscript.

Additional information

Correspondence and requests for materials should be addressed to E.D.

Reprints and permissions information is available at www.nature.com/reprints.

Publisher's note Springer Nature remains neutral with regard to jurisdictional claims in published maps and institutional affiliations.

Open Access This article is licensed under a Creative Commons Attribution-NonCommercial-NoDerivatives 4.0 International License, which permits any non-commercial use, sharing, distribution and reproduction in any medium or format, as long as you give appropriate credit to the original author(s) and the source, provide a link to the Creative Commons licence, and indicate if you modified the licensed material. You do not have permission under this licence to share adapted material derived from this article or parts of it. The images or other third party material in this article are included in the article's Creative Commons licence, unless indicated otherwise in a credit line to the material. If material is not included in the article's Creative Commons licence and your intended use is not permitted by statutory regulation or exceeds the permitted use, you will need to obtain permission directly from the copyright holder. To view a copy of this licence, visit <http://creativecommons.org/licenses/by-nc-nd/4.0/>.

© The Author(s) 2024